Gradient index metamaterials

D. R. Smith,[1,2,*] J. J. Mock,[1] A. F. Starr,[2,3] and D. Schurig[1]
[1]*Department of Electrical and Computer Engineering, Duke University, Box 90291, Durham, North Carolina 27708, USA*
[2]*Department of Mechanical and Aerospace Engineering, University of California, San Diego, La Jolla, California 92093, USA*
[3]*SensorMetrix, 5965 Pacific Center Boulevard, Suite 701, San Diego, California 92121-4323, USA*
(Received 4 July 2004; published 17 March 2005)

Metamaterials—artificially structured materials with tailored electromagnetic response—can be designed to have properties difficult or impossible to achieve with traditional materials fabrication methods. Here we present a structured metamaterial, based on conducting split ring resonators (SRRs), which has an effective index of refraction with a constant spatial gradient. We experimentally confirm the gradient by measuring the deflection of a microwave beam by a planar slab of the composite metamaterial over a range of microwave frequencies. The gradient index metamaterial may prove an advantageous alternative approach to the development of gradient index lenses and similar optics, especially at higher frequencies. In particular, the gradient index metamaterial we propose may be suited for terahertz applications, where the magnetic resonant response of SRRs has recently been demonstrated.

DOI: 10.1103/PhysRevE.71.036609 PACS number(s): 41.20.−q, 42.25.−p, 42.70.−a

There have now been several demonstrations in which electromagnetic material response—either previously unobserved or otherwise difficult to achieve in conventional materials—has been obtained in artificially structured materials [1–4]. These recent demonstrations have shown the potential of artificial materials, often referred to as *metamaterials*, to significantly extend the range of material properties, enabling the potential for new physical and optical behavior, as well as unique electromagnetic devices.

An example of unusual metamaterial response can be found in *negative index metamaterials*, which possess simultaneously negative permittivity (ε) and permeability (μ) over a finite frequency band. The fundamental nature of negative refraction, hypothesized in 1968 by Veselago [5], has revealed the key role that metamaterials can play in materials physics, as negative index is a material property not available in previously existing materials.

The negative index metamaterials thus far demonstrated have been formed from periodic arrays of conducting elements, the size and spacing of which are much less than the wavelengths of interest. The shape of the repeated conducting element determines the electromagnetic response of the collective, which can be approximated as having an electric [6] or a magnetic [7,8] resonance. Application of effective-medium theory to the overall periodically patterned composite allows a description in terms of bulk isotropic or anisotropic ε and μ.

The split ring resonator (SRR), shown in the insets to Fig. 1, has become commonplace as the repeated element in metamaterials that exhibit magnetic properties. A single SRR responds to electromagnetic fields in a manner analogous to a magnetic "atom," exhibiting a resonant magnetic dipolar response. A medium composed of periodically positioned SRRs can be approximately characterized by the following frequency-dependent permeability μ:

$$\mu(\omega) = 1 - \frac{F\omega^2}{(\omega^2 - \omega_r^2) + i\omega\gamma}, \tag{1}$$

where ω_r is a resonant frequency determined by the SRR geometry, γ is the damping, and F is the filling factor. The SRR element is electromagnetically anisotropic, so that μ in Eq. (1) refers only to the x component of the permeability tensor. We assume throughout that the electromagnetic field propagates along the z axis (see Fig. 1), the applied magnetic field liies along the SRR (x) axis and electric field lies along the y axis in the SRR plane; in this configuration, only μ_x and ε_y are relevant to the wave propagation characteristics.

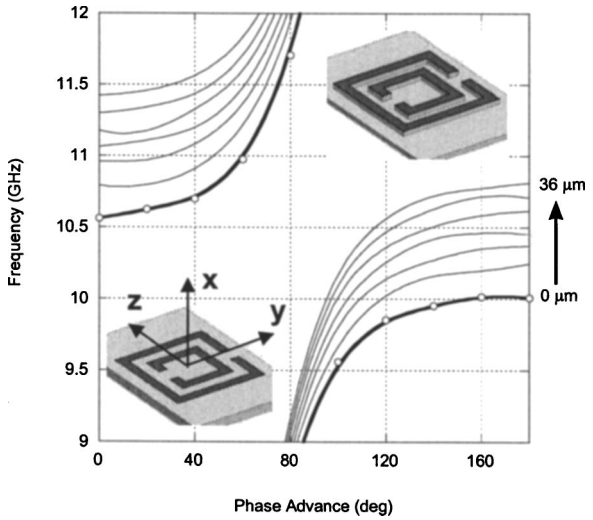

FIG. 1. Simulated dispersion curves for SRRs. The thicker black curve pair (including an upper and lower branch) corresponds to SRRs on a flat substrate (lower inset). The open circles indicate simulated phase advances. Subsequent pairs of curves correspond to cases in which the substrate has been removed around the SRR (upper inset). The depth of cut increases by 6 μm between each set of curves.

*Email address: drsmith@ee.duke.edu

The effective permittivity ε_y of the SRR medium has been shown to also be dispersive as a function of frequency [9]; however, this frequency-dependent behavior is minor at frequencies far away from the resonance, and approaches a constant in the limit of small cell size. Thus, we approximate here the permittivity as a constant over frequency.

We note that the SRR is actually a more complicated structure than our approximations would indicate, in that it inherently exhibits a coupled electric-magnetic response. The composite medium of SRRs is thus bianisotropic, generally requiring more parameters than just the ε and μ tensor components that we make use of here [10]. However, for our restricted choice of polarization and propagation direction relative to the SRR axis, those cross-coupling components are negligible and we are justified in describing the system with the two components specified [10–12].

In the recent work to date, metamaterials have been constructed from repeated unit cells containing identical elements, such that the resulting medium can be considered homogeneous in the sense that the averaged electromagnetic response does not vary over the structure. However, metamaterials whose averaged electromagnetic properties vary as a function of position can also be fabricated. Such materials are of interest, for example, as they can be utilized in a variety of applications, including lensing and filtering. Here we present a metamaterial based on SRRs, in which a spatially varying refractive index can be introduced by a slight change in the properties of each successive element along a direction perpendicular to the direction of propagation. We choose the parameters of the medium such that a relatively constant gradient in the index occurs along one axis of the metamaterial. The gradient is confirmed by beam deflection experiments.

While an SRR medium is known to have a predominantly magnetic response, this is not of direct interest here; rather, we are concerned with the phase advance of a wave propagating within the medium. For an isotropic medium, the refractive index $n(\omega)$ provides this information, with the phase advance over a distance d being nkd. For the anisotropic SRR medium, we can apply the usual isotropic definition anyway, $n(\omega)=\sqrt{\varepsilon(\omega)\mu(\omega)}$, with $\mu(\omega)$ given by Eq. (1) and $\varepsilon(\omega)$ approximated as constant. This provides the correct equivalent refractive index provided that the polarization is restricted as described above. The dispersion relation for these modes is $\omega=ck/n(\omega)$, which can be compared directly with that obtained from a numerical solution of Maxwell's equations for a single unit cell. To obtain the dispersion diagram numerically, we compute the eigenfrequencies for a single unit cell (Fig. 1, inset), applying periodic boundary conditions with zero phase advance in directions perpendicular to the propagation direction, and periodic boundary conditions with various phase advances in the propagation direction. The simulations are performed using a commercial finite-element based electromagnetic solver (HFSS, Ansoft). The resulting dispersion diagram, shown as the frequency versus the phase advance ϕ across a unit cell (black curve), reveals the expected resonant form. Specifically, there are two branches of propagating modes separated by a frequency band gap. The lower branch starts at zero frequency and ends at ω_r with a phase advance of 180°. The next branch begins at a frequency $\omega_{mp}=\omega_r/\sqrt{1-F}$ [7]. The propagation constant k can be found from $k=\phi/d$, where d is the size of the unit cell.

The resonant frequency of an SRR, ω_r, depends rather sensitively on the geometrical parameters and local dielectric environment for the SRR [7]. Since $\mu(\omega)$ depends strongly on ω_r [Eq. (1)], we see that relatively small changes to the basic repeated unit cell can result in substantial changes to the permeability of the composite, especially near the resonance. The change in index $n(\omega)=\sqrt{\varepsilon(\omega)\mu(\omega)}$ with change in resonant frequency can be calculated using Eq. (1). For convenience, we neglect damping; we also set $\varepsilon(\omega)=1$ as the primary role of the permittivity over the frequency band of interest will be to rescale the dispersion curves. At low frequencies ($\omega \ll \omega_r$), the index changes linearly with small changes in the resonance frequency, or

$$\Delta n \sim -\frac{\omega^2}{\omega_r^3}\Delta\omega_r, \tag{2}$$

whereas in the high-frequency limit ($\omega \gg \omega_r$), we find

$$\Delta n \sim -\frac{\omega_r}{\omega^2}\Delta\omega_r. \tag{3}$$

Assuming $\Delta\omega_r/\omega_r \ll 1$ and ignoring higher-order terms, we see that, for the model system described by Eq. (1), the gradient increases as the square of the frequency for $\omega \ll \omega_r$ and decreases as the inverse of the square of the frequency for $\omega \gg \omega_r$.

There are a variety of modifications to the SRR or its environment that can be used to introduce a variation in ω_r. The method we apply here is to adjust the depth of cut of the dielectric substrate material surrounding the SRR. This method is compatible with our sample fabrication, in which SRRs are patterned on copper clad circuit boards using a numerically controlled micromilling machine (described below). The removal of dielectric material from the region near the SRR ($\varepsilon \sim 3.8$ for FR4 circuit board) changes the local dielectric environment of the SRR, effecting a change in the resonance frequency.

In Fig. 1, we present several dispersion curves corresponding to SRR composites for various depths of substrate material around the SRR. The depth of substrate differs by 6 μm between successive dispersion curves. Figure 1 shows that ω_r shifts approximately *linearly* and monotonically with increasing depth of cut, up to 36 μ in depth. Further simulations, as well as the experimental results shown later, show the approximate linearity is valid to 240 μm.

Because the SRR exhibits a resonant frequency ω_r that increases linearly as a function of the substrate cut depth, it is a convenient element from which to design a gradient index metamaterial. In particular, if we form a metamaterial comprising a linear array of SRRs in which the substrate cut depth advances linearly as a function of cell number, ω_r will then also advance linearly as a function of cell number; that is, ω_r becomes linearly proportional to distance. Using this relationship in Eqs. (2) and (3), we see that the gradient of the index will thus be approximately constant as a function

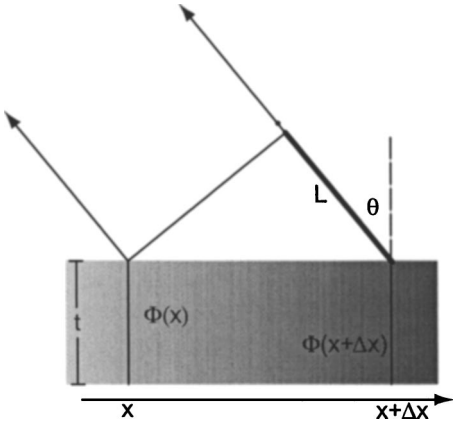

FIG. 2. Diagram showing the deflection of a wave by a structure whose refractive index possesses a gradient that is constant. Shading of the sample indicates the gradient in the index: lighter shading corresponds to a lower index value.

of distance, at least for frequencies far enough away from ω_r.

A constant gradient metamaterial can be experimentally confirmed by observing the deflection of a beam incident on a planar metamaterial slab whose index varies linearly (in a direction perpendicular to incident radiation). To calculate this deflection, we consider two normally incident but offset rays entering a gradient index planar slab of thickness t, as shown in Fig. 2. The rays will acquire different phase advances as they propagate through the slab. Assuming the two rays enter at locations x and $x+\Delta x$ along the slab face, then the acquired phase difference of the two beams traversing the slab,

$$\Phi(x+\Delta x)-\Phi(x)\sim kt\frac{dn}{dx}\Delta x, \tag{4}$$

must equal the phase advance across the path length marked L in Fig. 2. We thus have

$$\sin(\theta)\sim t\frac{dn}{dx}=t\frac{dn}{d\omega_r}\frac{d\omega_r}{d\delta}\frac{d\delta}{dx}, \tag{5}$$

which shows that for a material with a constant spatial gradient in index, the beam is uniformly deflected. Here, $\delta(x)$ is the depth of cut as a function of distance along the slab. This simplified analysis applies strictly to thin samples, as the phase fronts will otherwise not be uniform within the material. Note that $\Phi(x)$ is the phase shift across a slab of arbitrary thickness. If the slab is one unit cell in thickness, then for the SRR cell the phase shift will be ϕ as defined earlier.

In order to construct a constant gradient index metamaterial, the above analysis suggests that we form a linear array of SRRs, in which the substrate depth is a linearly increasing function of cell number in the direction perpendicular to the propagation. The resulting array should then deflect an incident beam by an angle that can be predicted by the dispersion diagrams in Fig. 1. To estimate this angle of deflection, we can take the difference between any two of the curves in Fig. 1 to find the gradient of the phase shift per unit cell. The phase shift per unit cell is proportional to the sine of the beam deflection angle that will be produced by a gradient

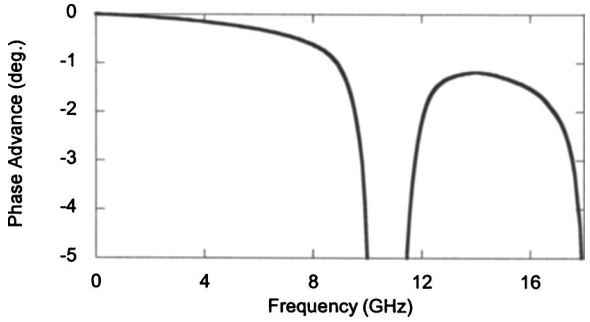

FIG. 3. Frequency vs phase difference per unit cell for the SRR material shown in Fig. 1, in which each successive cell differs by a 6 μm depth of cut.

index metamaterial slab one unit cell thick in the propagation direction. The resulting plot of phase advance as a function of frequency, obtained from the dispersion curve in Fig. 1, is shown in Fig. 3.

The curve in Fig. 3 is useful for calculating deflection angles only for frequencies where the gradient is constant, which can be determined, for example, by analyzing the differences between several of the dispersion curves of Fig. 1. Furthermore, near the resonant frequency on the low side, the absorption resonance leads to a region of anomalous dispersion where the simulation results (which do not take into account losses) are not valid. An additional complicating factor is that the analyzed structure is periodic, so that higher-order bands exist at frequencies greater than ω_r that are not described by Eq. (1). Nevertheless, Fig. 3 provides an indication that at frequencies above the band gap, per unit cell phase shifts of one degree or more should be obtainable from an SRR slab, one unit cell in thickness, in which each successive cell has an additional 6 μm of substrate dielectric removed relative to the previous cell.

To fabricate the gradient index metamaterial samples, a numerically controlled micromilling machine (ProtoMat 100, from LPKF, Oregon) was used to fabricate many short strips of SRRs, three or five unit cells in length. Single-sided copper-clad circuit board substrates were used (FR4, dielectric constant of 3.8, copper thickness of 0.017 mm). The unit cell for an individual SRR was 5.0 mm by 3.33 mm, with three SRRs patterned in the vertical direction such that the strips were 10 mm in height. The SRR design had identical parameters to those reported in [13]. For a typical sample, SRRs could be patterned by adjusting the tool bit to a depth just below the copper cladding level and removing all surrounding material that is not part of the SRR design.

To form the gradient index structure, the milling machine tool bit was lowered by two steps, or $\sim$6 μm, between the milling of successive strips. Strips were fabricated in this manner until the tool bit depth was nearly equal to the substrate thickness (0.25 mm). The strips were then cut out from the surrounding FR4 substrate and slotted for assembly. The process produced $\sim$35–40 SRR strips, each having SRRs with a surrounding substrate thickness that ranged from $\sim$0.250 mm to $\sim$0 mm in steps of 6 μm. Samples with strips of either three or five unit cell lengths in the propagation direction were fabricated, and composite metamaterials

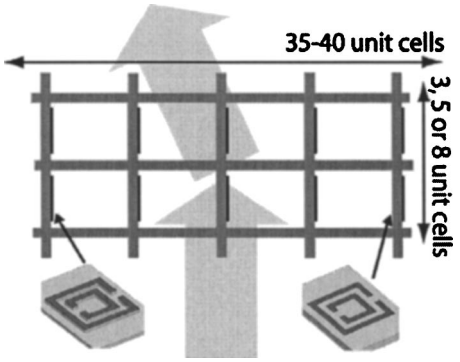

FIG. 4. A schematic depiction, as viewed from the top, of the gradient index metamaterial sample. The sample consists of circuit board strips containing patterned SRRs. The electric field is out of the plane of the figure, while the incident magnetic field is directed along the axes of the SRRs. The SRR positions are indicated by the darker lines in the figure, with the circuit board strips indicated by lighter gray lines.

assembled with roughly 40 strips (of three or five unit cell lengths) spaced one unit cell width (5 mm) apart. The strips were held together by slotted FR4 cross pieces from which all copper had been removed in a wine-crate assembly. The sample construction is indicated schematically in Fig. 4.

The resonance frequency of each individual SRR strip was measured in an angular resolved microwave spectrometer (ARMS) described previously [14]. The measured resonance frequencies of each strip (of the three-cell-thick SRR slab) versus the depth of cut are plotted in Fig. 5, where the linearity of the fabrication process is confirmed. The nominal difference in substrate thickness between subsequent milling passes was 6 μm. Note that at two depths there are breaks from the linearity; these deviations from linearity coincide with tool bit changes on the milling machine, indicating some lack of reproducibility in repositioning the mill at the nominal zero cut depth position. The resulting linearity, however, proved to be sufficient for the deflection experiment.

The composite gradient index samples were measured in

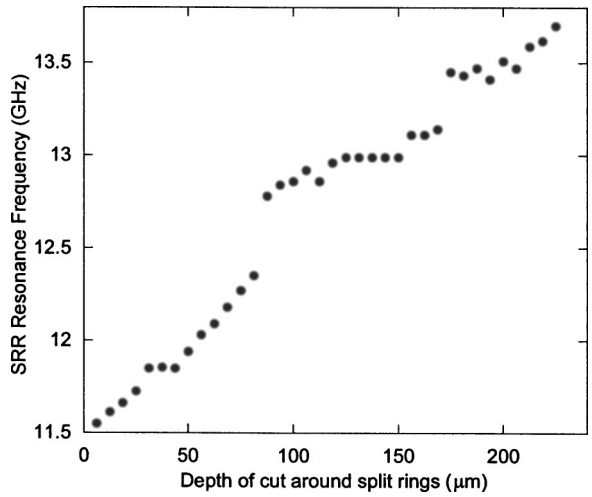

FIG. 5. Resonant frequency vs substrate depth for the machined SRR samples.

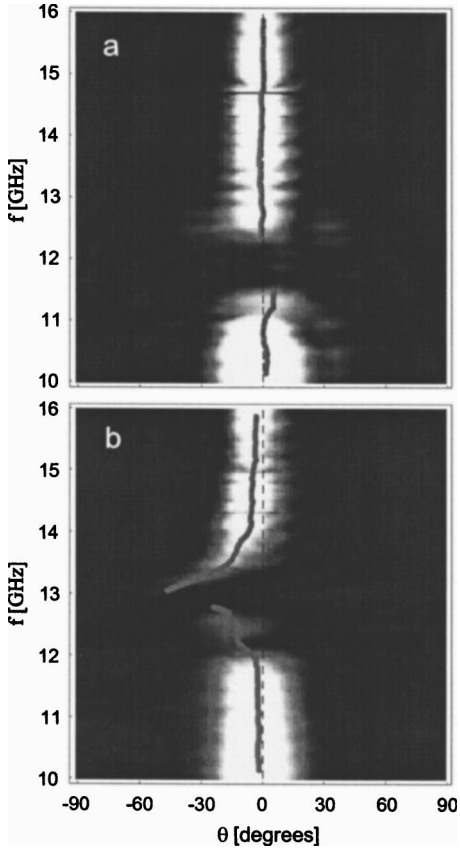

FIG. 6. Angular maps vs frequency of the power emerging from (a) an SRR sample, five unit cells in thickness, with no index gradient and (b) an SRR sample, eight unit cells in thickness, with linear gradient in the direction transverse to the incoming beam. The gray curve superimposed summarizes the peak power at each frequency.

the ARMS apparatus. To confirm the gradient in the sample, a microwave beam was directed normally onto the face of the sample (as in Fig. 2), and the power detected as a function of angle at a radius 40 cm away. As in previous measurements on metamaterial samples, the experiment was carried out in a planar waveguide—an effectively two-dimensional geometry in which the electric field is polarized between two conducting (aluminum) plates [14].

In Fig. 6, we present a map of the transmitted power versus angle of detection, as a function of the frequency of the incident microwave beam. Two samples are compared in the figure: Fig. 6(a) shows a control sample consisting of a five-cell-deep SRR metamaterial, where each SRR strip is identical (no gradient). The plot in Fig. 6(a) shows transmission at frequencies corresponding to pass bands, and a frequency region of attenuation corresponding to where the permeability is negative. As can be seen from the figure, the microwave beam exits the sample without deflection, centered about zero degrees.

In Fig. 6(b), we present the results of a measurement on an eight-cell-thick (in propagation direction) gradient index sample, formed by combining the three- and five-cell samples together. The angular deviation is evident in the figure, especially at the high-frequency side of the gap region,

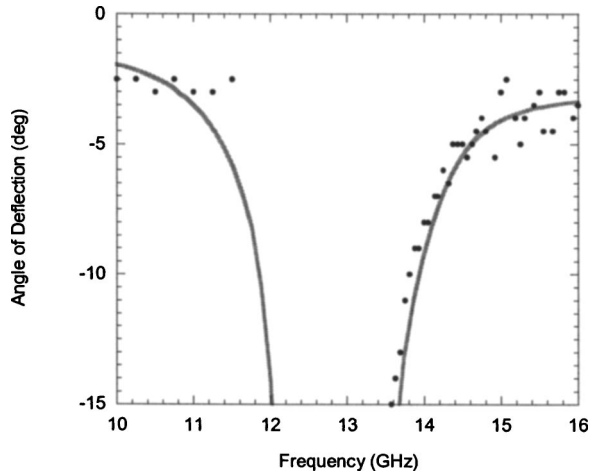

FIG. 7. Measured angle of deflection (black circles) of a gradient index SRR slab, eight unit cells in thickness. The gray curves are taken from those shown in Fig. 3, but have been translated in frequency so that the calculated and the measured band-gap regions overlap.

where a characteristic tail can be seen in agreement with that predicted in Fig. 3. The qualitative aspects of the curve are in agreement with the theory and simulations above, except that there is weaker evidence of deflection on the low-frequency side of the gap. This lack of symmetry, however, is expected, as the lower-frequency side corresponds to the resonance, where the absorption (neglected in the dispersion diagrams) is strongest.

A detailed comparison of the measured and calculated angle of deflection versus frequency is shown in Fig. 7 for the eight-cell-thick gradient index metamaterial. The curves correspond to the gradient determined from Fig. 3, while the black circles are measured points. A frequency translation was applied to the dispersion curve to make the calculated band gap coincident with the band gap measured in the actual structure; no other fitting or adjustments were performed. The excellent agreement shown in Fig. 7 attests to the precision of the fabrication process, as illustrated in Fig. 5. The agreement also provides evidence that even a single unit cell can be described as having a well-defined refractive index, since the interpretation of this effect depends on a refractive index that varies controllably from cell to cell within the structure.

Figures 6 and 7 show the practicality of designed spatially dispersive structures. In this case, a linear gradient has been introduced that has the effect of uniformly deflecting a beam by an angle adjustable by design. We find it convenient to work with the SRR system, as the properties of SRRs are now well established. In particular, the resonance frequency of the SRR is relatively easy to identify, can be easily tuned by slightly modifying the parameters of the unit cell, and can be used to roughly parametrize the entire frequency dependence of the SRR. While not the only method for introducing a gradient, the gradient index SRR structure shows the feasibility of creating yet another unique type of metamaterial by combining macroscopic elements.

An evident application of the gradient index metamaterial is in gradient index lenses. A parabolic (as opposed to linear) distribution of index in the slab along an axis perpendicular to the direction of wave propagation results in a structure that focuses radiation rather than deflecting it [15]. Common examples of such gradient index lenses include radial gradient index rod lenses, used at optical frequencies, and Luneberg lenses, used at microwave frequencies. Gradient index rod lenses use optical glass materials that are ion-doped via thermal diffusion. This process can produce only modest variations of the refractive index (less than 0.2), and is limited to fairly small diameter rods (less than 1 cm) [16]. Luneberg spherical or hemispherical lenses, which require the fairly wide index range of $n=1$ to $n=2$, can be implemented as stepped index devices with no particular size limitation [15]. Both devices employ gradients in the dielectric permittivity only, and thus have limited impedance matching to the surrounding media.

Gradient index metamaterials may provide a useful alternative approach to the development of optics. The advantages of both traditional and planar lenses formed from artificially patterned media, for example, have been demonstrated at radio and microwave frequencies [17]. With the increased range of material response now identified in metamaterials, including negative refractive index, considerably more flexibility and improved performance from such devices should be possible [18]. Gradient index metamaterials that include magnetic permeability gradients, for example, could be used to develop materials whose index varies spatially but which remains matched to free space. Moreover, with the recent demonstration of SRRs at THz frequencies [19], the gradient index metamaterial should be realizable at higher frequencies.

This work was supported by DARPA, through an ONR MURI (Contract No. N00014-01-1-0803). A.F.S. and D.R.S. also acknowledge support from DARPA through ARO (Contract No. DAAD19-00-1-0525).

[1] D. R. Smith, W. Padilla, D. C. Vier, S. C. Nemat-Nasser, and S. Schultz, Phys. Rev. Lett. **84**, 4184 (2000).
[2] R. A. Shelby, D. R. Smith, and S. Schultz, Science **292**, 79 (2001).
[3] C. G. Parazzoli, R. B. Greegor, K. Li, B. E. C. Koltenbah, and M. Tanielian, Phys. Rev. Lett. **90**, 107401 (2003).
[4] A. A. Houck, J. B. Brock, and I. L. Chuang, Phys. Rev. Lett. **90**, 137401 (2003).
[5] V. G. Veselago, Sov. Phys. Usp. **10**, 509 (1968).
[6] J. B. Pendry, A. J. Holden, W. J. Stewart, and I. Youngs, Phys. Rev. Lett. **76**, 4773 (1996).
[7] J. B. Pendry, A. J. Holden, D. J. Robbins, and W. J. Stewart, IEEE Trans. Microwave Theory Tech. **47**, 2075 (1999).
[8] R. W. Ziolkowski and F. Auzanneau, J. Appl. Phys. **82**, 3192

(1997).
[9] T. Koschny, P. Markos, D. R. Smith, and C. M. Soukoulis, Phys. Rev. E **68**, 065602 (2003).
[10] R. Marques, F. Medina, and R. Rafii-El-Idrissi, Phys. Rev. B **65**, 144440 (2002).
[11] N. Katsarakis, T. Koschny, M. Kafesaki, E. N. Economou, and C. M. Soukoulis, Appl. Phys. Lett. **84**, 2943 (2004).
[12] T. Koschny, M. Kafesaki, E. N. Economou, and C. M. Soukoulis, Phys. Rev. Lett. **93**, 107402 (2004).
[13] R. A. Shelby, D. R. Smith, S. C. Nemat-Nasser, and S. Schultz, Appl. Phys. Lett. **78**, 4 (2001).
[14] A. F. Starr, P. M. Rye, J. J. Mock, and D. R. Smith, Rev. Sci. Instrum. **75**, 820 (2004).
[15] E. W. Marchland, *Gradient Index Optics* (Academic Press, New York, 1978).
[16] H. Hashizume, K. Hamanaka, A. C. Graham, and X. F. Zhu, Proc. SPIE **4437**, 26 (2001).
[17] J. D. Krauss, *Antennas*, 2nd ed. (McGraw-Hill, Boston, 1988), Chap. 14.
[18] D. Schurig and D. R. Smith, e-print physics/0403147.
[19] T. J. Yen, W. J. Padilla, N. Fang, D. C. Vier, D. R. Smith, J. B. Pendry, D. N. Basov, and X. Zhang, Science **303**, 1494 (2004).